Influence of Reactant Polarity on the Course of the Inverse-Electron-Demand Diels−Alder Reaction. A DFT Study of Regio- and Stereoselectivity, Presence of Lewis Acid Catalyst, and Inclusion of Solvent Effects in the Reaction between Nitroethene and Substituted Ethenes

Luis R. Domingo,* Manuel Arnó, and Juan Andrés[†]

Departamento de Química Orgánica, Universidad de Valencia, Dr. Moliner 50, 46100 Burjassot, Valencia, Spain, and Departament de Ciències Experimentals, Universitat Jaume I, Apartat 224, 12080, Castelló, Spain

Received February 22, 1999

The molecular mechanisms for the inverse-electron-demand Diels−Alder reactions between nitroethene and three substituted ethenes (propene, methyl vinyl ether, and dimethylvinylamine) to give the corresponding nitroso cycloadducts have been characterized with density functional theory methods using the B3LYP/6-31G* calculational level. On the basis of stability arguments and molecular orbital analysis relative rates, regioselectivity, and stereoselectivity, the presence of Lewis acid catalyst modeled by the BH_3 system and the inclusion of solvent effects as a function of the nature of substituent in the dienophile fragment are analyzed and discussed. The ortho attack mode presents transition structures more stable than the meta one. For the former, reactivity, endo selectivity, and asynchronicity are enhanced with the increase of the electron-releasing character of the substituent on dienophile fragment. The reaction between nitroethene and propene has dissymmetric concerted transition structures associated with a pericyclic process, while the reaction between nitroethene and dimethylvinylamine takes place along an asynchronous transition structure corresponding to a nucleophilic attack to nitroethene, with concomitant ring closure and without participation of zwitterionic intermediates. For the most unfavorable meta attack modes, the reactions have synchronous mechanisms that are not sensible to the substitution on the dienophile system. For the ortho channels, the inclusion of Lewis acid catalyst and solvent effects contributes to the charge-transfer process from the substituted ethenes to nitroethene and rate acceleration, as well as a significant increase of the endo stereoselectivity.

Introduction

The Diels−Alder (DA) reaction is one of the most useful synthetic reactions, and its overwhelming importance is well-known and thoroughly documented in organic chemistry. Its usefulness arises from its versatility and from its remarkable selectivity; many synthetic routes to cyclic compounds are made possible through DA reactions, which can involve a large variety of dienes and dienophiles. By varying its structural nature, many different types of compounds can be built up.[1] The DA reaction mechanism has been the subject of controversy and stimulated debate since its discovery;[2] the general question of whether [4 + 2] cycloadditions are concerted or stepwise processed is of considerable current interest. It may take place by synchronous or asynchronous concerted mechanisms or by a stepwise mechanism.[2,3]

A normal DA reaction requires a electron-rich diene and an electron-poor dienophile,[4] while an inverse-electron-demand DA reaction has the opposite requirements and has been the subject of recent investigations.[5] In both types of processes, the substitution on both diene and dienophile makes the reactions have asynchronous mechanisms. Furthermore, the presence of the electron-releasing (or -withdrawing) groups on the diene and electron-withdrawing (or -releasing) groups on the dienophile, which can stabilize electric charges of either sign, allows that the molecular mechanism can be stepwise, via a zwitterionic intermediate.[6,7]

[†] Universitat Jaume I.

(1) (a) Hammer, J. *1,4-Cycloaddition Reactions, the Diels−Alder in Heterocyclic Synthesis*; Academic Press: New York, 1967. (b) Boger, D. L.; Weinreb, S. M. *Hetero Diels−Alder Methodology in Organic Synthesis*; Academic Press: Orlando, FL, 1987. (c) Carruthers, W. *Cycloaddition Reactions in Organic Synthesis*; Pergamon: Oxford, 1990. (d) Oppolzer, W.; Weinreb, S. M.; Boger, D. L.; Roush, W. R. *Comprehensive Organic Synthesis: Combining C−C p-Bonds*; Pergamon Press: Oxford, 1991; Vol. 5, Chapters 4.1−4.4.

(2) (a) Dewar, M. J. S.; Olivella, S.; Stewart, J. J. P. *J. Am. Chem. Soc.* **1986**, *108*, 5771. (b) Bach, R. D.; MacDouall, J. J. W.; Schlegel, H. B.; Wolber, G. C. *J. Org. Chem.* **1989**, *54*, 2931. (c) Houk, K. N.; Li, Y.; Evanseck, J. D. *Angew. Chem., Int. Ed. Engl.* **1992**, *31*, 682. (d) Houk, K. N.; González, J.; Li, Y. *Acc. Chem. Res.* **1995**, *28*, 81.

(3) (a) Bernardi, F.; Bottoni, A.; Field, M. J.; Guest, M. F.; Hillier, I. H.; Robb, M. A.; Venturini, A. *J. Am. Chem. Soc.* **1988**, *110*, 3050. (b) Tietze, L. F.; Fennen, J.; Anders, R. *Angew. Chem., Int. Ed. Engl.* **1989**, *28*, 1371. (c) Tran Hau Dau, M. E.; Flament, J.-P.; Lefour, J.-M.; Riche, C.; Grierson, D. S. *Tetrahedron Lett.* **1992**, *33*, 2343. (d) Coxon, J. M.; McDonald, D. Q. *Tetrahedron Lett.* **1992**, *33*, 3673. (e) Jursic, B. S.; Zdravkovski, Z. *J. Chem. Soc., Perkin Trans. 2* **1994**, 1877. (f) Jursic, B. S.; Zdravkovski, Z. *THEOCHEM* **1994**, 90. (g) Carpenter, J. E.; Sosa, C. P. *THEOCHEM* **1994**, *311*, 325. (h) Suarez, D.; Gonzalez, J.; Sordo, T. L.; Sordo, J. A. *J. Org. Chem.* **1994**, *59*, 8085. (i) Storer, J. W.; Raimondi, L.; Houk, K. N. *J. Am. Chem. Soc.* **1994**, *116*, 9675.

(4) (a) Fleming, I. *Frontier Orbitals and Organic Chemical Reactions*; John Wiley and Sons: New York, 1976. (b) Sauer, J.; Sustmann, R. *Angew. Chem., Int. Ed. Engl.* **1980**, *19*, 778.

(5) (a) Boger, D. L.; Corbett, W. L.; Curran, T. T.; Kasper, A. M. *J. Am. Chem. Soc.* **1991**, *113*, 1713. (b) Markó, I. E.; Evans, G. R. *Tetrahedron Lett.* **1994**, *35*, 2767. (c) Pugnaud, S.; Masure, D.; Hallé, J.-C.; Chaquin, P. *J. Org. Chem.* **1997**, *62*, 8687. (d) Liu, J.; Niwayama, S.; You, Y.; Houk, K. N. *J. Og. Chem.* **1998**, *63*, 1064.

10.1021/jo990331y CCC: $18.00
Published on Web 07/21/1999

Scheme 1

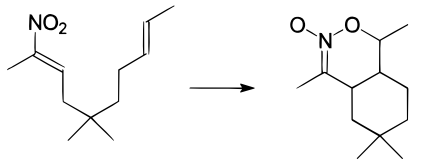

Scheme 2

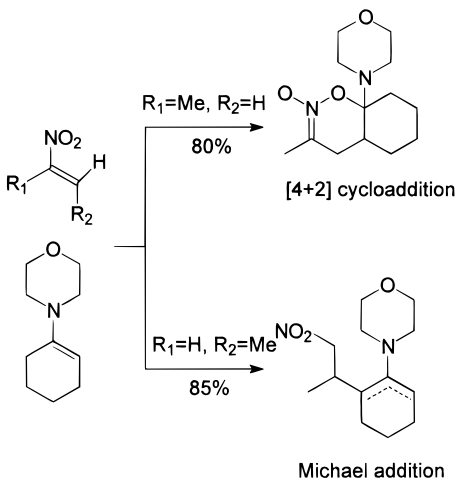

Many theoretical and experimental studies have been carried out to rationalize the DA reactions of the great variety of dienes and dienophiles. In particular, the cycloaddition reactions of heterodienes with olefins constitute versatile and direct methods for the construction of heterocyclic compounds. Several reports have appeared that describe the use of simple or substituted alkenes in hetero-DA reactions with nitroalkenes as a heterodiene.[8] Because of the low reactivity of the simple alkenes, the thermal reactions require high temperature or the presence of Lewis acids.[9] An example is the intramolecular cycloaddition shown in Scheme 1.[9a] The use of oxygen-containing dienophiles also requires Lewis acids.[8] A few examples of simple thermal cycloadditions of enol ethers and nitroalkenes have been reported, and in all cases the nitronates were isolated in moderate yields.[5c,10] In addition, the powerful nucleophilicity of enamines makes the addition to nitroalkenes take place without the presence of Lewis acids. The isolation of secondary products, which can be explained by an initial Michael addition, suggests the participation of zwitterionic intermediates in the mechanism of the reaction (see Scheme 2).[11]

In view of these precedents, and as a part of our research program devoted to the study of molecular mechanisms of the cycloaddition reactions that take place

Scheme 3

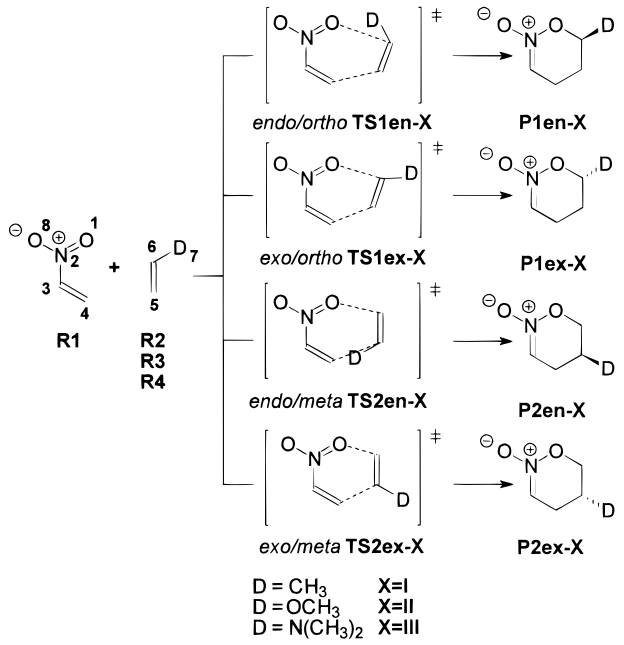

via asynchronous mechanisms,[7,12] we present herein the results of a theoretical study on the inverse-electron-demand DA reactions of nitroethene, **R1**, and three substituted ethenes: propene, **R2**, methyl vinyl ether, **R3**, and dimethylvinylamine, **R4**, to give the corresponding cycloadducts (see Scheme 3). Our purpose is to contribute to a better understanding of the influence of substituents and the origins of the regio- and stereochemical outcomes and to shed light on the mechanistic details of this important reaction. Lewis acid catalyst and solvent effects have been also included in order to clarify their role on the nature of the molecular mechanisms.

Computational Methods

In recent years, theoretical methods based on the density functional theory[13] (DFT) have emerged as an alternative to traditional ab initio methods in the study of structure and reactivity of chemical systems. The DA reaction has been the object of several density functional studies,[7,14] showing that functionals that include gradient corrections and hybrid functionals, such as B3LYP,[15] together the 6-31G* basis set,[16] lead to potential energy barriers (PEBs) in good agreement with the experimental results. Thus, in the present study geometrical optimizations of the stationary points along the

(6) (a) Sustmann, R.; Sicking, W. *J. Am. Chem. Soc.* **1996**, *118*, 12562. (b) Sustmann, R.; Tappanchai, S.; Bandmann, H. *J. Am. Chem. Soc.* **1996**, *118*, 12555.

(7) Domingo, L. R.; Picher, M. T.; Zaragozá, R. J. *J. Org. Chem.* **1998**, *63*, 9183.

(8) Denmark, S. E.; Thorarensen, A. *Chem. Rev.* **1996**, *96*, 137.

(9) (a) Denmark, S. E.; Cramer, C. J.; Sternberg, J. A. *Helv. Chim. Acta* **1986**, *69*, 1971. (b) Denmark, S. E.; Moon, Y.-C.; Cramer, C. J.; Dappen, M. S.; Senanayake, C. B. W. *Tetrahedron* **1990**, *46*, 7373.

(10) Bäckvall, J.-E.; Karlsson, U.; Chinchilla, R. *Tetrahedron Lett.* **1991**, *32*, 5607.

(11) Risaliti, A.; Forchiassin, M.; Valentin, E. *Tetrahedron* **1968**, *24*, 1889.

(12) (a) Domingo, L. R.; Jones, R. A.; Picher, M. T.; Sepúlveda-Arqués, J. *Tetrahedron* **1995**, *51*, 8739. (b) Domingo, L. R.; Picher, M. T.; Andrés, J.; Moliner, V.; Safont, V. S. *Tetrahedron* **1996**, *52*, 10693. (c) Domingo, L. R.; Picher, M. T.; Andrés, J.; Safont, V. S. *J. Org. Chem.* **1997**, *62*, 1775.

(13) (a) Parr, R. G.; Yang, W. *Density Functional Theory of Atoms and Molecules*; Oxford University Press: New York, 1989. (b) Ziegler, T. *Chem. Rev.* **1991**, *91*, 651.

(14) (a) Stanton, R. V.; Merz, K. M. *J. Chem. Phys.* **1994**, *100*, 434. (b) Baker, J.; Muir, M.; Andzelm, J. *J. Chem. Phys.* **1995**, *102*, 2036. (c) Jursic, B.; Zdravkovski, Z. *J. Chem. Soc., Perkin Trans. 2* **1995**, 1223. (d) Goldstein, E.; Beno, B.; Houk, K. N. *J. Am. Chem. Soc.* **1996**, *118*, 6036. (e) Branchadell, V. *Int. J. Quantum Chem.* **1997**, *61*, 381. (f) Sbai, A.; Branchadell, V.; Ortuño, R. M.; Oliva, A. *J. Org. Chem.* **1997**, *62*, 3049. (g) Branchadell, V.; Font, J.; Moglioni, A. G.; Ochoa de Echaguen, C.; Oliva, A.; Ortuno, R. M.; Veciana, J.; Vidal Gancedo, J. *J. Am. Chem. Soc.* **1997**, *119*, 9992. (h) Domingo, L. R.; Arnó, M.; Andrés, J. *J. Am. Chem. Soc.* **1998**, *120*, 1617.

(15) (a) Becke, A. D. *J. Chem. Phys.* **1993**, *98*, 5648. (b) Lee, C.; Yang, W.; Parr, R. G. *Phys. Rev. B* **1988**, *37*, 785.

(16) Hehre, W. J.; Radom, L.; Schleyer, P. v. R.; Pople, J. A. *Ab initio Molecular Orbital Theory*; Wiley: New York, 1986.

potential energy surface (PES) were carried out by means of B3LYP/6-31G* calculation method. The stationary points were characterized by frequency calculations in order to verify that minima (reactants, intermediates, and products) and transition structures (TSs) have zero and one imaginary frequency, respectively. The optimizations were carried out using the Berny analytical gradient optimization method.[17] The transition vector (TV),[18] i.e., the eigenvector associated to the unique negative eigenvalue of the force constants matrix, has been characterized. All calculations were carried out with the Gaussian 94 suite of programs.[19] Optimized geometries of all the structures are available from the authors. The electronic structures of stationary points were analyzed by the natural bond orbital (NBO) method.[20]

It is well-known that the use of Lewis acids can lead to significant changes in the nature of the molecular mechanism in comparison with the uncatalyzed processes. This fact has led to a huge amount of experimental work, in which a wide variety of this type of catalysts have been employed.[21] The effect of catalysts in DA reactions has also been the object of several semiempirical[22] and ab initio[23,24] theoretical studies. These works predict that the catalyst produces a notable increase in the dissymmetry of the TS. Experimentally, it is well-known that the reactions between nitroalkenes and alkenes or enol ethers are performed in the presence of Lewis acids. Thus, the effects of the Lewis acid catalyst were considered by studying these reactions with BH_3 as a computational model. This system has been used by different authors to model the presence of Lewis acids with good results.[24] The BH_3 can be coordinated to an oxygen atom of the nitro group belonging to the nitroethene **R1** in an endo or exo orientation. Previous calculations of DA reactions render that the exo BH_3-coordinated is predicted to be favored over the endo one.[24c] This arrangement has been selected in the present study.

The vast majority of chemical reactions are performed in solution, and as solvent effects can yield valuable information about the reaction mechanism, the need to increase our knowledge about interactions between solvent a solute remains crucial. The solvent effects have been considered by B3LYP/6-31G* optimizations of stationary points using a relatively simple self-consistent reaction field (SCRF)[25] method, based on the Onsager model,[26] in which the solvation energy is calculated from the electrostatic energy between the solute, modelized as a dielectric sphere of radius a_o, and the solvent, described as a continuum of dielectric constants (ϵ). The solvent used in the experimental work is dichloromethane. Therefore, we have used the dielectric constant at 298.0 K, $\epsilon = 8.93$.[27] This methodology has been used successfully for the study of related cycloaddition reactions.[28]

Results and Discussion

In the first section, energetic aspects, geometrical parameters of TSs and their electronic structure in terms of bond orders and natural charges will be analyzed. In the second section, the role of the Lewis acid catalyst will be rationalized. Finally, the solvent effects will be presented and discussed.

(a) Gas-Phase Calculations. There are four possible reaction pathways depending on the approach of the substituted ethene with respect to the nitro group of the heterodiene and on the conformation of the latter: ortho/endo, ortho/exo, meta/endo, and meta/exo. We will denote the corresponding transition structures as **TS1en-X**, **TS1ex-X**, **TS2en-X,** and **TS2ex-X**, where **TS1** and **TS2** are related to the ortho and meta regioisomer pathways, **en** and **ex** are related to the endo and exo stereoisomer pathways, and **X** = **I**, **II**, and **III** are related to the electron-releasing groups on the substituted ethene, $-CH_3$, $-OCH_3$, and $-N(CH_3)_2$, respectively (see Scheme 3). Endo/exo and ortho/meta arrangements are two pairs of stereoisomers and regioisomers, respectively. From these TSs, the related minima associated with the final cycloadducts can be obtained, **P1en-X**, **P1ex-X**, **P2en-X,** and **P2ex-X**; endo/exo arrangement corresponds to a pair of enantiomers.

Some selected geometrical parameters of the calculated TSs are shown in Figure 1, while Table 1 reports the values of relative energies for the stationary points. In Figure 2a, a schematic representation of the different reaction pathways for the reaction **R1** + **R3** is depicted. For the methyl vinyl ether a transoid conformation of the methyl group with respect to the vinyl ether system has been selected.[5d]

An exhaustive exploration of the PES allows us to find several molecular complexes (MCs) associated with early stages of the cycloaddition and situated on a very flat region that controls the access to the different reactive channels. The formation of these MCs may take place in different arrangements of the reactants, with a large distance between the diene and dienophile fragments (3.3−3.5 Å), which correspond to van der Waals complexes.[6a,29] Their presence in a very shallow minima on PES with low relative stability with respect the reactant fragments in the range of 1.2−3.5 kcal/mol does make it very difficult to determine the location of MC associated to each reactive channel. However, the fact that this energetic range is lower than the relative energies between the corresponding TSs (see Figure 2a) allows us the use of PEBs defined as the difference of energy between the different TSs and the corresponding reactant

(17) (a) Schlegel, H. B. *J. Comput. Chem.* **1982**, *3*, 214 (b) Schlegel, H. B. *Geometry* Optimization on Potential Energy Surface. in *Modern Electronic Structure Theory*; Yarkony, D. R., Ed.; World Scientific Publishing: Singapore, 1994.

(18) (a) McIver, J. W. J.; Komornicki., A. *J. Am. Chem. Soc.* **1972**, *94*, 2625. (b) McIver, J. W. J. *Acc. Chem. Res.* **1974**, *7*, 72.

(19) Frisch, M. J.; Trucks, G. W.; Schlegel, H. B.; Gill, P. M. W.; Johnson, B. G.; Robb, M. A.; Cheeseman, J. R.; Keith, T.; Petersson, G. A.; Montgomery, J. A.; Raghavachari, K.; Al-Laham, M. A.; Zakrzewski, V. G.; Ortiz, J. V.; Foresman, J. B.; Cioslowski, J.; Stefanov, B. B.; Nanayakkara, A.; Challacombe, M.; Peng, C. Y.; Ayala, P. Y.; Chen, W.; Wong, M. W.; Andres, J. L.; Replogle, E. S.; Gomperts, R.; Martin, R. L.; Fox, D. J.; Binkley, J. S.; Defrees, D. J.; Baker, J.; Stewart, J. P.; Head-Gordon, M.; Gonzalez, C.; Pople, J. A. *Gaussian 94*; Gaussian, Inc.: Pittsburgh, PA, 1995.

(20) (a) Reed, A. E.; Weinstock, R. B.; Weinhold, F. *J. Chem. Phys.* **1985**, *83*, 735. (b) Reed, A. E.; Curtiss, L. A.; Weinhold, F. *Chem. Rev.* **1988**, *88*, 899.

(21) Santelli, M.; Pons, J.-M. *Lewis Acids and Selectivity in Organic Synthesis*; CRC Press: Boca Raton, 1996.

(22) (a) Branchadell, V.; Oliva, A.; Bertrán, J. *THEOCHEM* **1985**, *113*, 197. (b) Branchadell, V.; Oliva, A.; Bertrán, J. *THEOCHEM* **1985**, *120*, 85. (c) Branchadell, V.; Oliva, A.; Bertrán, J. *THEOCHEM* **1986**, *120*, 117. (d) Domingo, L. R.; Picher, M. T.; Andrés, J. *J. Phys. Org. Chem.* **1999**, *12*, 24.

(23) (a) Jursic, B. S.; Zdravkovski, Z. *J. Org. Chem.* **1995**, *59*, 7732. (b) Yamabe, S.; Dai, T.; Minato, T. *J. Am. Chem. Soc.* **1995**, *117*, 10994. (c) Dai, W.-M.; Lau, C. W.; Chung, S. H.; Wu, D.-Y. *J. Org. Chem.* **1995**, *60*, 8128. (d) García, J. I.; Mayoral, J. A.; Salvatella, L. *J. Am. Chem. Soc.* **1996**, *118*, 11680. (e) García, J. I.; Martínez-Merino, V.; Mayoral, J. A.; Salvatella, L. *J. Am. Chem. Soc.* **1998**, *120*, 2415.

(24) (a) Birney, D. M.; Houk, K. N. *J. Am. Chem. Soc.* **1990**, *112*, 4127. (b) McCarrick, M. A.; Wu, Y.-D.; Houk, K. N. *J. Org. Chem.* **1993**, *58*, 3330. (c) Venturini, A.; Joglar, J.; Fustero, S.; Gonzalez, J. *J. Org. Chem.* **1997**, *62*, 3919.

(25) (a) Tomasi, J.; Persico, M. *Chem. Rev.* **1974**, *94*, 2027. (b) Simkin, B. Y.; Sheikhet, I. *Quantum Chemical and Statistical Theory of Solutions-A Computational Approach*; Ellis Horwood: London, 1995.

(26) (a) Wong, M. W.; Frisch, M. J.; Wiberg, K. B. *J. Am. Chem. Soc.* **1990**, *112*, 4776. (b) Wong, M. W.; Wiberg, K. B.; Frisch, M. J. *J. Chem. Phys.* **1991**, *95*, 8991.

(27) David, R. L. *CRC Handbook of Chemistry and Physics*, 76th ed.; CRC Press: Boca Raton: FL, 1996.

(28) Cativiela, C.; García, J. I.; Mayoral, J. A.; Salvatella, L. *Chem. Soc. Rev.* **1996**, *25*, 209.

(29) Suarez, D.; Sordo, J. A. *Chem. Commun.* **1998**, 385.

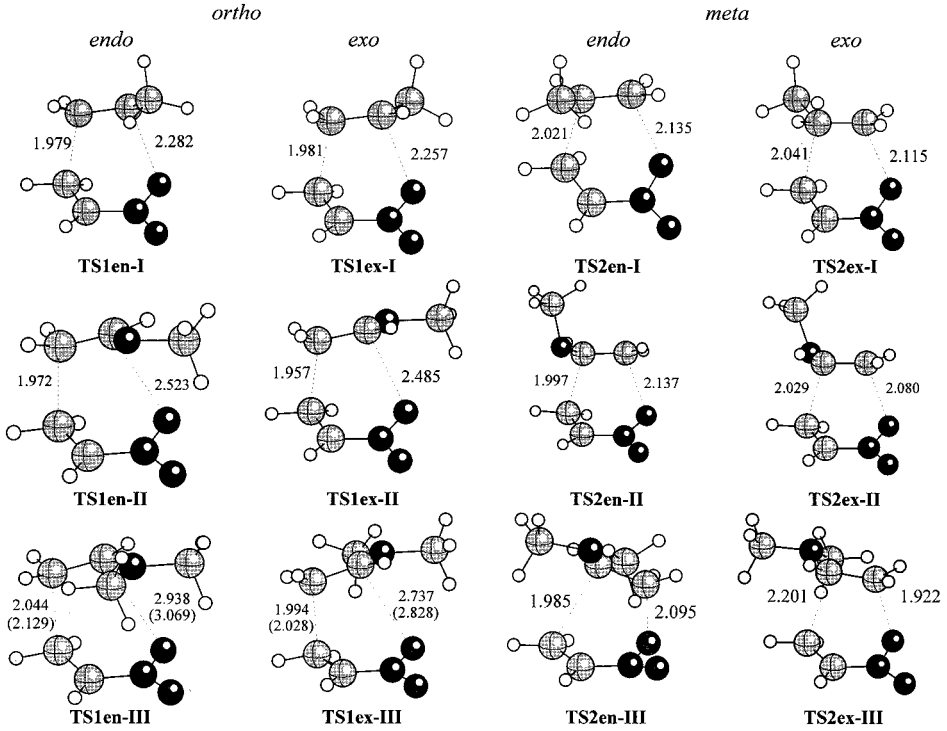

Figure 1. Transition structures corresponding to the uncatalyzed reactions between nitroethene **R1** and propene **R2**, methyl vinyl ether **R3**, and dimethylvinylamine **R4**. The values of the bond lengths directly involved in the processes are given in angstroms. The values in parentheses correspond to the reaction in dichloromethane.

Table 1. Relative Energies (kcal/mol) for the Stationary Points of the Cycloaddition Reactions between R1 and R2,[a] R1 and R3,[b] and R1 and R4[c]

R1 + R2	0.0	**R1 + R3**	0.0	**R1 + R4**	0.0
MC1en-I	−1.9	**MC1en-II**	−3.8	**MC1en-III**	−3.6
TS1en-I	21.4	**TS1en-II**	9.7	**TS1en-III**	4.7
TS1ex-I	20.7	**TS1ex-II**	12.3	**TS1ex-III**	9.1
TS2en-I	25.6	**TS2en-II**	28.6	**TS2en-III**	30.6
TS2ex-I	25.8	**TS2ex-II**	28.6	**TS2ex-III**	31.6
				TS3−III	10.3
P1en-I	−21.7	**P1en-II**	−26.9	**P1en-III**	−19.4
P1ex-I	−21.7	**P1ex-II**	−26.9	**P1ex-III**	−19.4
P2en-I	−21.2	**P2en-II**	−17.6	**P2en-III**	−12.6
P2ex-I	−21.2	**P2ex-II**	−17.6	**P2ex-III**	−12.6
				ZW−III	10.1

[a] Total energy of **R1** + **R2** is −400.995462 au. [b] Total energy of **R1** + **R3** is −476.198331 au. [c] Total energy of **R1** + **R4** is −495.650252 au.

fragments to discuss the energetic results. The most stable MCs along the four reactive channels, **MC1en-X**, are included in Table 1.

(i) Energies. All reactions are exothermic processes, in the range of −12.6 to −26.9 kcal/mol. The four reactive channels render two pairs of enantiomers with identical energies, the ortho cycloadducts (**P1en-X** and **P1ex-X**) being more stable than the meta ones (**P2en-X** and **P2ex-X**).

Analysis of the PEBs for the TSs reveals that the ortho approaches are favored over the meta ones; the **TS1en-X** and **TS1ex-X** are more stable than **TS2en-X** and **TS2ex-X**, in the range of 4.4−24.5 kcal/mol. The PEBs of the ortho TSs decrease in the order **I**, **II**, and **III**; while an opposite behavior is found for the meta ones. Therefore, there is a clear regioselectivity for this type of chemical reaction. The stereoselectivity measured as the difference of PEBs between the endo and exo TSs for the more favorable ortho attack is dependent also on the substituent on the dienophile fragment; the differences in energy between **TS1en-X** and **TS1ex-X** are −0.7, 2.7, and 4.4 kcal/mol for the systems **I**, **II**, and **III**, respectively.

The endo stereoselectivity found for the systems **R3** and **R4** along the ortho attacks can be explained by means of two favorable interactions, which can overcome the steric repulsive interactions involved in endo TSs. The first one is due to a hyperconjugative anomeric-type interaction between the lone pair on the O1 oxygen atom of the nitro group and the σ^*CO and σ^*CN molecular orbitals of the enol and enamine, respectively, that appears in the endo TSs.[5a,d] This behavior does not appear at system **R2** and can justify that **TS1ex-I** is slightly more stable than **TS1en-I**, because of the steric hindrance present in the endo TS.[5d] The second one is due to a favorable Coulombic interaction that appears between the substituent on the ethene and the nitro group along the endo approach, which are developing electric charges of either sign.[6a]

All attempts to find zwitterionic intermediates on reactive PES preceding the formation of the final cycloadducts were unsuccessful. A small displacement of the nuclear coordinates at the corresponding TSs toward the reaction products leads directly to cycloadducts.

However, the powerful nucleophicity of enamines can open the possibility of a Michael-type addition for the reaction between dimethylvinylamine, **R4**, and nitroethene, **R1**. Therefore, the presence of a zwitterionic intermediate cannot be discarded. This intermediate can afford the final cycloadduct along a stepwise mechanism or give Michael-type adducts along subsequent reactions.[7] Although a zwitterion could not be found starting with the synperiplanar conformation, there remains the possibility that such species might be generated in an extended conformation. Thus, the approach of the enamine **R4** to nitroethene **R1** in an antiperiplanar conforma-

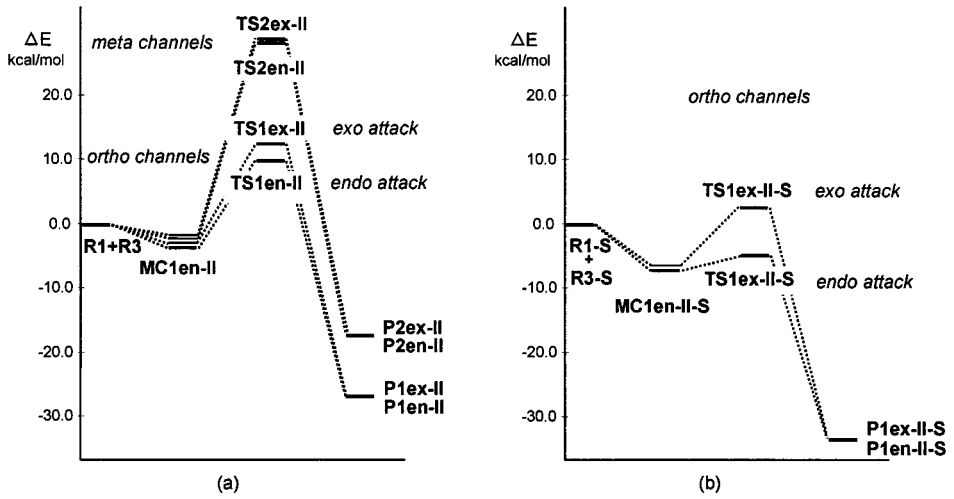

Figure 2. Schematic representation of the different energy profiles for the reaction between nitroethene **R1** and methyl vinyl ether **R3** (a) in the gas phase and (b) including Lewis acid catalyst and solvent effects.

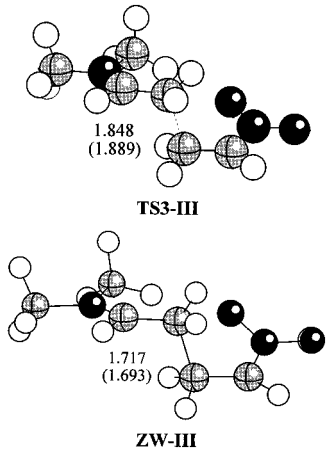

Figure 3. Transition structure **TS3-III** and zwitterion **ZW-III** corresponding to the antiperiplanar attack of the dimethyl vinylamine **R4** to nitroethene **R1**. The values of the bond lengths directly involved in the processes are given in angstroms. The values in parentheses correspond to the reaction in dichloromethane.

tion allows the formation of the zwitterion intermediate **ZW-III**, via the transition structure **TS3-III**. The geometries of the **TS3-III** and **ZW-III** are displayed in Figure 3. The PEB for the formation of the zwitterion **ZW-III** (10.3 kcal/mol) is larger than for the formation of the cycloadduct **P1en-III** via **TS1en-III** (4.7 kcal/mol); the PEB for the reverse step, **ZW-III** → **R1** + **R4**, is only 0.2 kcal/mol. The formation of zwitterion **ZW-III** cannot be ruled out, but this entity is expected to be very short-lived, since its cleavage requires a PEB of the same order of magnitude as that of the rotational barriers. Under these conditions, the zwitterion can be formed in an open conformation that does not allow the ring closure, giving back to the reactants. However, for more complex nitroalkene and enamine systems (see Scheme 2), for which steric hindrances can appear along the synperiplanar cycloaddition process, the two pathways can be competitive.

For the nonexpected meta attacks, the difference of energies between **TS2en-X** and **TS2ex-X** is quite low. Therefore, there is no stereoselectivity along these pathways.

(ii) Geometries. In the case of the uncatalyzed process, all ortho TSs correspond with asynchronous reaction pathways. The extent of the asynchronicity can be measured by means of the difference between the distances of the bonds that are being formed in the reaction, i.e., Δr = d(O1−C6) − d(C4−C5) and Δr = d(O1−C5) − d(C4−C6) for the ortho TSs, **TS1en-X** and **TS1ex-X**, and the meta TSs, **TS2en-X** and **TS2ex-X**, respectively. For the former TSs, the Δr value increases in the order **I** < **II** < **II** (see Figure 1), following the rise of the electron-releasing character of the substituent on the ethene. For the meta TSs, the Δr values are independent of the substitution on the ethene.

The presence of a heteroatom in the **R3** and **R4** systems with a lone pair increases the dissymmetry of the two bonds being formed in the TSs; the α bonds being formed to the methoxy and amino groups are longer that those β to these groups. For the substituted ethene, the β carbon is more nucleophilic than the α one. Consequently, there is more bond formation at the β center in the TSs. The **TS1en-III** has the largest difference, Δr = 0.9. A separation of ca. 3.0 Å at one end of the TS and 2.0 Å at the other leads to appreciable covalent interaction only at the unsubstituted side;[6a,7] the corresponding cycloadduct is formed directly from this TS without involving intermediates.

Since some reactive channels present very dissymmetric TSs, diradical structures could in principle be involved. This has been ruled out by obtaining the wave functions of all TSs with unrestricted DFT theory.[12b,30] UB3LYP/6-31G* calculation predicts the same TSs as the restricted B3LYP/6-31G*, indicating that the restricted DFT solutions are stable, allowing us to rule out the presence of more stable diradical species.

The dominant TV components correspond to the O1−C6 and C4−C5 bond distances for the ortho isomer TSs and the O1−C5 and C4−C6 bond distances for the meta ones, which are associated with the two σ bonds that are being formed in these cycloaddition processes. For the ortho TSs, the values of C4−C5 components increase and the values of the O1−C6 components decrease in the

(30) Kahn, S. D.; Hehre, W. J.; Pople, J. A. *J. Am. Chem. Soc.* **1987**, *109*, 1871.

Table 2. Wiberg Bond Orders at the Transition Structures TS1en-X, TS1ex-X, TS2en-X, and TS2ex-X (X = I, II, and III)

	O1−N2	N2−C3	C3−C4	C4−C5	C5−C6	O1−C6	C6−D7
TS1en-I	1.28	1.17	1.41	0.50	1.45	0.23	1.07
TS1ex-I	1.27	1.17	1.41	0.50	1.45	0.24	1.07
TS1en-II	1.30	1.17	1.40	0.51	1.41	0.12	1.15
TS1ex-II	1.29	1.17	1.39	0.52	1.40	0.13	1.13
TS1en-III	1.36	1.15	1.42	0.47	1.40	0.04	1.34
TS1ex-III	1.32	1.15	1.41	0.50	1.37	0.07	1.31
	O1−N2	N2−C3	C3−C4	C4−C6	C5−C6	O1−C5	C6−D7
TS2en-I	1.25	1.19	1.42	0.47	1.45	0.31	1.03
TS2ex-I	1.24	1.19	1.44	0.45	1.45	0.32	1.03
TS2en-II	1.25	1.18	1.42	0.47	1.44	0.31	0.94
TS2ex-II	1.23	1.19	1.44	0.45	1.43	0.34	0.94
TS2en-III	1.16	1.21	1.45	0.38	1.36	0.46	1.09
TS1ex-III	1.17	1.22	1.46	0.38	1.35	0.45	1.09

order **I**, **II**, and **III**; this fact can be related with the dissymmetry observed for these TSs.

The imaginary frequency values for the ortho TSs are in the range of 319−493i cm^{-1}, while those for the meta TSs are in the range of 544−614i cm^{-1}. For the ortho TSs there is a decreasing of the imaginary frequency value, which is parallel to the increase of the asynchronicity of the process. Moreover, these values are lower for the endo TSs than for the exo ones. The asynchronicity in the bond formation process is also shown by the fact that the imaginary frequencies of the ortho TSs have a larger participation on the motion of the C4−C5 bond being formed than for the O1−C6 one.

(iii) Bond Order and Charge Analysis. A more balanced measure of the extent of bond-formation or bond-breaking processes along a reaction pathway is provided by the concept of bond order (BO). This theoretical tool has been used to study the molecular mechanism of chemical reactions.[31] To follow the nature of these processes, the Wiberg bond indices[32] have been computed by using the NBO analysis as implemented in Gaussian94. The results are included in Table 2.

For the more favorable ortho TSs, **TS1en-X** and **TS1ex-X**, the C4−C5 BO values are constants (around 0.50), while O1−C6 BO values decrease along the series (0.23, 0.12, and 0.04, for the endo approaches). This fact can be related with the electron-releasing character of the substituent on C6, which increases the nucleophilic character of the substituted ethene, increasing the asynchronicity of the process. Thus, for **TS1en-III** the O1−C6 BO indicates an unappreciable covalent interaction between these atoms.[7] The increase of the C6−D7 (D = C, O, N) BO at the ortho TSs (1.07, 1.15, and 1.34, for the endo approaches) points out a π-delocalization of the lone pair of heteroatoms of the dienophile fragment in **TS1en-II** and **TS1en-III**, which increases the nucleophilic character of the dienophile.

For the meta TSs, the C4−C6 and O1−C5 BO values (in the range of 0.38−0.47 and 0.31−0.45, respectively) indicate a minor change in the asynchronicity with the substitution on C6 center than in the ortho TSs. Moreover, the C6−D7 (D = C, O, N) BO values (in the range 0.94−1.09) are not dependent on substituent effects.

The BO analysis shows the change of asynchronicity for the ortho reactive channels. For the system **R2**, the cycloaddition takes place via a concerted process where the two σ bonds are simultaneously but dissymmetrically formed. For the system **R4**, the reaction takes place via an asynchronous process, in which the C4−C5 bond is being formed, while the O1 and C6 atoms are not yet being bonded at the TS. For the nonexpected meta reactive channels, the BO analysis affords synchronous TSs associated with pericyclic processes.

Table 3. Natural Population Analysis of the Negative Charge (in au) Transfered from the Substituted Ethene to Nitroethene for the Transition Structures TS1en-X, TS1ex-X, TS2en-X, and TS2ex-X (X = I, II, and III)

TS1en-I	0.21	**TS1en-II**	0.34	**TS1en-III**	0.41
TS1ex-I	0.24	**TS1ex-II**	0.33	**TS1ex-III**	0.39
TS2en-I	0.21	**TS2en-II**	0.19	**TS2en-III**	0.30
TS2ex-I	0.22	**TS2ex-II**	0.20	**TS2ex-III**	0.31

One possibility to test the existence and relative importance of all the aforementioned interactions lie in the values of natural population analysis (NPA). NPA also supports an increase of the polar nature of the ortho TSs to go from **I** to **III** systems (Table 3). The negative charge transfer from the substituted ethene to nitroethene are 0.21e (**TS1en-I**), 0.24e (**TS1ex-I**), 0.34e (**TS1en-II**), 0.33e (**TS1ex-II**), 0.41e (**TS1en-III**), and 0.39e (**TS1ex-III**), indicating that the nature of these TSs can be seen to occur from some zwitterionic character. The amount of the charge transfer in these TSs is mainly controlled by electron-releasing character of the substituent on C6, which favors the electron-transfer process, and agree with the increase of the asynchronicity in the bond-formation process. Finally, the charge transfer in **TS1en-III** is similar to that in **TS3-III** (0.44e), showing the similar electronic nature of both TSs.

The charge analysis also supports the Coulombic interactions that appear in the endo TSs **TS1en-II** and **TS1en-III**. These favorable interactions allow an increase of the charge-transfer process for the endo TSs relative to exo ones, because of a larger participation of the lone pair of the heteroatoms along the endo cycloaddition processes.

(iv) Frontier Molecular Orbital Analysis. These reactions appear to be under frontier control, being the FMO model capable of explaining the substituent effects for these inverse-electron-demand cycloadditions. In Figure 4, the substituent effects for the present cycloadditions is rationalized by using a FMO analysis. The main HOMO−LUMO interaction occurs between the LUMO of the diene ($LUMO_{diene}$) and the HOMO of the dienophile ($HOMO_{dienophile}$). The $LUMO_{diene}$ of the nitroethene **R1** is quite low in energy, and this approach at first seems

(31) (a) Varandas, A. J. C.; Formosinho, S. J. F. *J. Chem. Soc., Faraday Trans. 2* **1986**, 282. (b) Lendvay, G. *THEOCHEM* **1988**, *167*, 331. (c) Lendvay, G. *J. Phys. Chem.* **1989**, *93*, 4422. (d) Lendvay, G. *J. Phys. Chem.* **1994**, *98*, 6098.

(32) Wiberg, K. B. *Tetrahedron* **1968**, *24*, 1083.

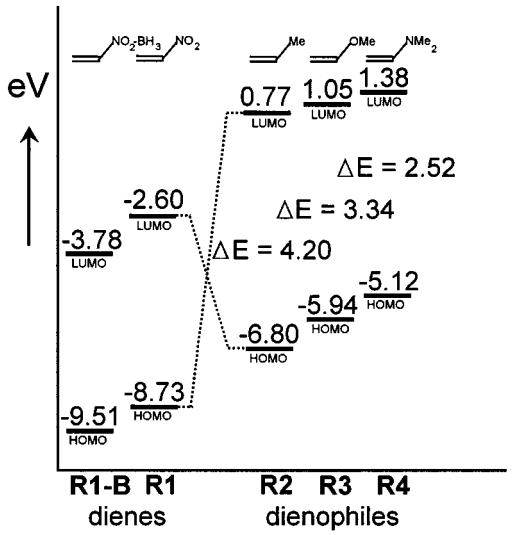

Figure 4. Frontier molecular orbitals on the cycloaddition reactions between diene, **R1**, and dienophiles, **R2**, **R3**, and **R4**. **R1-B** is **R1** coordinated with BH_3 Lewis acid catalyst.

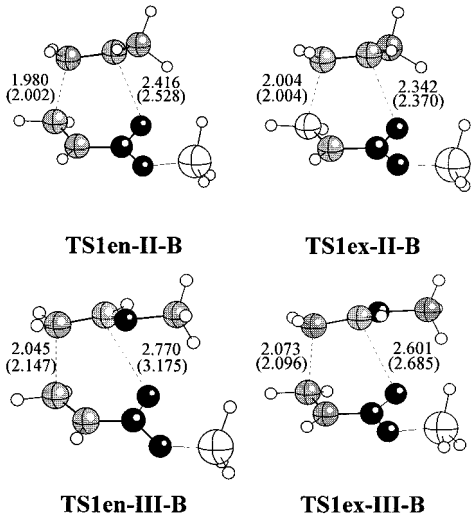

Figure 5. Transition structures corresponding to the *ortho* pathways for the catalyzed reactions between nitroethene, **R1-B**, and propene, **R2**, and methyl vinyl ether, **R3**. The values of the bond lengths directly involved in the processes are given in angstroms. The values in parentheses correspond to the catalyzed reaction in dichloromethane.

reasonable. If these are the dominant interactions, then the relative energies should decrease on going from **R2** to **R4**, since the $HOMO_{dienophile}$ energy rises in this series. For an inverse-electron-demand DA cycloaddition, the presence of a electron-releasing group in the dienophile and electron-withdrawing substituents in the diene leads to a contraction of the more relevant ($HOMO_{dienophile}$) − ($LUMO_{diene}$) energy separation, and the reactivity increases consequently. The regioselectivity can be also rationalized in terms of FMO interactions along the ortho and meta channels. The essential difference between both reaction pathways concerns the relative orientation of the two fragments. Along the ortho reactive mode, there is an arrangement in which an optimized overlap occurs between the HOMO of the dienophile fragment (associated with the π system of the substituted ethene) and the LUMO of the diene fragment (associated with π^* system of the nitroethene). This fact justifies the regioselectivity found in this type of cycloaddition; the most favorable reactive channel corresponds with the ortho pathway.

(b) Lewis Acid Catalyst. As stated in the Introduction, the reactions between nitroalkenes and nonactived alkenes take place only in the presence of Lewis acids, while the reactions using actived alkenes can be carried out without the presence of Lewis acids. Therefore, only the effect of Lewis acid catalyst on the systems **I** and **II** is studied. Because of the large energetic difference between ortho and meta TSs, only the ortho reaction pathways have been studied, taking into account the presence of Lewis acid and solvent effects. The geometries of BH_3-coordinated TSs **TS1en-I-B**, **TS1ex-I-B**, **TS1en-II-B**, and **TS1ex-II-B** are depicted in Figure 5, while Table 4 presents the values of the relative energies corresponding to these TSs.

The presence of Lewis acid decreases the PEBs for these cycloadditions in the range of 5.0−6.7 kcal/mol, compared with those for the uncatalyzed processes. This behavior of the Lewis acid catalysts has been found in previous studies on related DA reactions,[24] and it can be understood in terms of a stronger interaction between the $HOMO_{dienophile}$ − $LUMO_{diene}$. Figure 4 shows the decrease of the $LUMO_{diene}$ energy (0.78 eV) for the BH_3-coordinated nitroethene, **R1-B**, compared with the nitroethene **R1**; this fact decreases the $HOMO_{dienophile}$ − $LUMO_{diene}$ energy gap, in agreement with the lowering of PEBs for the catalyzed reactions.

Table 4. Relative Energies (kcal/mol) for the Stationary Points of the Ortho Pathways of the BH_3-Catalyzed Cycloaddition Reactions between R1-B and R2[a] and R1-B and R3[b]

R1-B + R2	0.0	**R1-B + R3**	0.0
MC1en-I-B	−2.1	**MC1en-II-B**	−4.9
TS1en-I-B	13.8	**TS1en-II-B**	2.6
TS1ex-I-B	14.1	**TS1ex-II-B**	4.1

[a] Total energy of **R1-B** + **R2** is −427.633508 au. [b] Total energy of **R1-B** + **R3** is −502.836377 au.

There is a more noticeable change on structural features for the BH_3-coordinated TSs. The Lewis acid catalyst enhances significantly the dissymmetry of TSs, due to the increase of the O1−C6 distance. This fact is also observed in the analysis of the BOs. The O1−C6 BOs for **TS1en-I-B** and **TS1en-II-B** are 0.18 and 0.08, respectively; the BO value for **TS1en-II-B** is similar to that for the asynchronous **TS1en-III** (0.09).

The NPA at **TS1en-I-B** and **TS1en-II-B** shows an increase of charge transfer (0.05e) from the substituted ethenes, **R2** or **R3**, to BH_3-coordinated nitroalkene, **R1-B**, relative to uncatalyzed processes. However, the most noticeable effect of the Lewis acid as catalyst is the delocalization of the negative charge that is being transferred at TSs. A partial charge analysis at **TS1en-I-B** and **TS1en-II-B** shows that the BH_3 fragment accepts 0.27e and 0.28e, respectively, of the 0.31e and 0.37e transferred to heterodiene system. This fact allows a stabilization of the corresponding TSs, lowering the PEBs associated with these cycloadditions and increasing the asynchronicity of the processes.

The Lewis acid catalyst has an opposite role in the stereoselectivity found for these catalyzed reactions. While for the reaction between **R1-B** and **R2** the endo channel is the most favorable pathway, for the reaction

Table 5. Relative Energies (kcal/mol) for the Stationary Points of the Ortho Pathways and Zwitterion Intermediate, Including the Solvent Effects (Dichoromethane, $\epsilon = 8.93$), of the Cycloaddition Reactions between R1-S and R2-S,[a] R1-S and R3-S,[b] and R1-s and R4-S[c] (Note that for R4, the Lewis Acid Catalyst, BH_3, Is Not Included)

R1-S + R2-S	0.0	**R1-S + R3-S**	0.0	**R1-S + R4-S**	0.0
MC1en-I-S	−4.7	**MC1en-II-S**	−7.0	**MC1en-III-S**	−3.8
TS1en-I-S	7.7	**TS1en-II-S**	−4.6	**TS1en-III-S**	2.1
TS1ex-I-S	13.7	**TS1ex-II-S**	3.0	**TS1ex-III-S**	7.7
				TS3-III-S	9.4
				ZW-III-S	8.7

[a] Total energy of **R1-S** + **R2-S** is −427.635515 au. [b] Total energy of **R1-S** + **R3-S** is −502.838512 au. [c] Total energy of **R1-S** + **R4-S** is −495.651029 au.

between **R1-B** and **R3** there is a decrease in the endo stereoselectivity. These facts can be explained by the Coulombic stabilization that appears in the endo approach. While for the system **R2** the presence of the Lewis acid increases the charge-transfer process and consequently the favorable Coulombic interaction, for the system **R3** the delocalization of the transferred charge on BH_3 decreases the negative charge in the nitro group and an opposite effect appears.

The role of the Lewis acid catalyst can be understood as an increase of the electrophilic character of the nitroethene due to a stabilization of the corresponding TS through a delocalization of the negative charge that is being transferred along the nucleophilic attack of the substituted ethene.

(c) Solvent Effect Calculations. Solvent effects on DA reactions are well-known[33] and have received considerable attention, especially in the past few years, because these studies can clarify the role of the solvent on related pericyclic reactions.[12b,28,34] The next step in our investigation was to study the solvent effects on the basic features of the molecular mechanism for these cycloadditions. For systems **R2** and **R3**, the BH_3-coordinated TSs have been fully optimized including the solvent effects, while for the system **R4** the uncatalyzed ortho TSs have been chosen. Thus, six TSs have been studied: **TS1en-I-S**, **TS1ex-I-S**, **TS1en-II-S**, **TS1ex-II-S**, **TS1en-III-S**, and **TS1ex-III-S**.

The geometries of these TSs, including the selected geometrical parameters, are depicted in Figures 1 and 5, while Table 5 presents the relative energies. Inclusion of the solvent effects appears to be both qualitatively and quantitatively significant. Solvent effects decrease the PEBs for all TSs in the range 0.4−7.2 kcal/mol, in agreement with the polar character of TSs. Inclusion of solvent effects affords a negative PEB for **TS1en-II-S** (−4.6 kcal/mol) because of a large stabilization of this TS relative to the reactants. However, if the formation of the molecular complex **MC1en-II-S** is considered, this PEB becomes positive (2.4 kcal/mol).

Table 6. Natural Population Analysis of the Negative Charge (in au) Transfered from the Substituted Ethene to Nitroethene[a] for the Transition Structures TS1en-X-S and TS1ex-X-S (X = I, II, and III) in Dichoromethane

TS1en-I-S	0.35	**TS1en-II-S**	0.39	**TS1en-III-S**	0.41
TS1ex-I-S	0.30	**TS1ex-II-S**	0.36	**TS1ex-III-S**	0.40

[a] For **I** and **II** nitroethene is BH_3-coordinated.

Solvent effects lead to an increase in the *endo/exo* stereoselectivity through a preferential solvatation of the endo TSs over their corresponding exo counterparts. This is in qualitative agreement with the increase in the *endo/exo* selectivity with the polarity of the solvent experimentally observed for related reactions.[28] This fact is more remarkable for the system **R2**, since inclusion of the Lewis acid and solvent effects changes the stereoselectivity found in the gas phase, being **TS1en-I-S** 6.0 kcal/mol more stable than **TS1ex-I-S**.

Formation of the zwitterion **ZW-III-S** seems to be independent of solvent effects; **TS1en-III-S** is more stabilized than **TS3-III-S** when the solvent effects are included. This fact allows us to discard the formation of **ZW-III-S** for the reaction between **R1-S** and **R4-S**.

The NPA for the charge-transfer process of these TSs are given in Table 6. An analysis of these results points out that the most remarkable effect is the increase of the charge transfer for **TS1en-I-S** relative to **TS1en-I-B** (0.08e). This fact is in agreement with the strong decrease of the PEB and the larger increase of dissymmetry in the bond formation found for **TS1en-I-S**. Moreover, a comparison between the charge-transfer for **TS1en-S** and **TS1ex-I-S** also points out that this process is more favorable along endo attack because of the favorable Coulombic interactions that appear in the endo approach.

Conclusions

In the present work, we have carried out a theoretical study of the molecular mechanisms for the inverse-electron-demand DA cycloadditions of nitroethene with three substituted ethenes using DFT (B3LYP/6-31G*) methods. The PESs have been explored, and four reactive pathways, ortho/endo, ortho/exo, meta/endo and meta/exo, have been characterized. Relative rates, regioselectivity, and stereoselectivity have been analyzed and discussed as a function of the polar nature of the substituent on the ethene fragment. The role of the Lewis acid catalyst modeled by BH_3 system and solvent effects has been included for approach this theoretical study to the experimental conditions.

The energy ordering shows that the ortho channels are more favorable than the meta ones. For the ortho pathways, there is a relation between the nature of the molecular mechanism and the polar character of the substituted ethene; increasing the electron-releasing character of the substituent enhances the asynchronicity and the charge-transfer process as well as a significant decrease of the potential energy barrier. These results agree with those expected from frontier molecular orbital theory.

The molecular mechanism of the reaction between nitroethene and propene corresponds with a pericyclic process, while the reaction between nitroethene and dimethylvinylamine is a nucleophilic attack with concomitant ring closure and without intervention of a zwitterionic intermediate.

(33) (a) Pindur, U.; Lutz, G.; Otto, C. *Chem. Rev.* **1993**, *93*, 741. (b) Li, C.-J. *Chem. Rev.* **1993**, *93*, 2023. (c) Blokzijl, W.; Engberts, J. B. F. N. *Angew. Chem., Int. Ed. Engl.* **1993**, *32*, 1545.

(34) (a) Blake, J. F.; Jorgensen, W. L. *J. Am. Chem. Soc.* **1991**, *113*, 7430. (b) Ruiz-López, M. F.; Assfeld, X.; García, J. I.; Mayoral, J. A.; Salvatella, L. *J. Am. Chem. Soc.* **1993**, *115*, 8780. (c) Jorgensen, W. L.; Lim, D.; Blake, J. F.; Severance, D. L. *J. Chem. Soc., Faraday Trans.* **1994**, *90*, 1727. (d) Davidson, M. M.; Hillier, I. H.; Hall, R. J.; Burton, N. A. *J. Am. Chem. Soc.* **1994**, *116*, 9294. (e) Cativiela, C.; Dillet, V.; García, J. I.; Mayoral, J. A.; Ruiz-López, M. F.; Salvatella, L. *THEOCHEM* **1995**, *331*, 37.

Inclusion of the Lewis acid catalyst and solvent effects decrease the PEBs and increase the asynchronicity of these processes as well as the charge-transfer process from the substituted ethene to nitroethene. The Lewis acid catalyst has an opposite role in the stereoselectivity for the catalyzed reactions. While for the reaction with propene inclusion of the Lewis acid catalyst changes the endo/exo stereoselectivity with the endo channel being the most favorable pathway, for the reaction with methyl vinyl ether there is a decrease in the endo stereoselectivity. Finally, inclusion of solvent effects leads to an increase in the *endo/exo* stereoselectivity, through a preferential solvation of the endo TS over their corresponding exo counterparts.

As a consequence of the results described in this paper, we recommend to include models for the Lewis acid catalyst and solvent effects at a high computational level (B3LYP/6-31G*) to study theoretically the reactive pathways, in particular TSs, related with the regioselectivity and stereoselectivity of the cycloaddition reactions involving polar species.

Acknowledgment. This work was supported by research funds provided by the Conselleria de Cultura Educació i Ciéncia, Generalitat Valenciana (Project GV97-CB-11-86). All calculations were performed on a Cray-Silicon Graphics Origin 2000 with 64 processors of the Servicio de Informática de la Universidad de Valencia. We are most indebted to this center for providing us with computer capabilities.

Supporting Information Available: Tables giving the total energies for the stationary points of the cycloaddition reactions between nitroethene **R1** and propene **R2**, methyl vinyl ether **R3**, and dimethyl vinylamine **R4**, *in a vacuum*, for the BH_3-catalyzed reactions and for the reactions in dichloromethane. Tables giving the imaginary frequency, the Hessian unique negative eigenvalue, and the main TV components and their corresponding geometric parameters for all TSs corresponding to the cycloaddition reactions between nitroethene **R1** and propene **R2**, methyl vinyl ether **R3**, and dimethylvinylamine **R4**. This material is available free of charge via the Internet at http://pubs.acs.org.

JO990331Y